UiT The Arctic University of Norway

Design considerations for a dust collector on mesospheric rocket

Henriette Trollvik, Ingrid Mann, Ove Havnes, Sveinung Olsen, and Yngve Eilertsen

UiT-The Arctic University of Norway, Department of Physics and Technology, Norway (hmtrollvik@gmail.com)

EGU – General Assembly 2020

Abstract

Meteors ablation is a source of dust particles in the upper atmosphere. The remnants of meteor ablation that prevail in the mesosphere condense to nm-sized particles, denoted as Meteoric Smoke Particles (MSPs). Theory suggests that MSPs act as condensation nuclei for ice particles in the summer mesosphere, which form during summer months around the mesopause at high and mid latitudes. The MSP and the ice particles are related to mesospheric phenomena such as the Noctilucent Clouds, Polar Mesospheric Summer and Winter Echoes (PMSE/PMWE). However, due to their altitude location, the only means of in situ measurement is with rocket experiments. There have been several attempts over the years to collect MSPs with probes on rockets, but no conclusive results have been reported so far. Most attempts aimed to collect MSPs directly.

UiT have proposed a new sample collector, the MEteoric Smoke Sampler (MESS) (Havnes et al. 2015). The instrument is designed to collect large ice particles, since the airflow conditions at the rocket payload affect them less than smaller MSPs. After evaporation of the ice component, the refractory MSPs that are contained in the ice remain on the collections surface. We report on the progress of the work that has focused on the design of the detector and simulation of the entry and impact of dust onto the detector. Estimations of the collection efficiency of the instrument and the impact energy at the collecting area are presented.

If we target sampling of PMC particles based on a recent model by Kiliani et al. With the discussed instrument design and its dimensions given in the presentation we expect to be able to collect and bring back to the laboratory of the order of 10^{14} to 10^{15} amu of refractory MSP particles. The estimate basis on the assumption that the ice component are melting and the flow conditions in the instruments are for typical atmospheric pressures at 85 km. We point out we had an erroneous estimate in the abstract.

Instrument design

- The MESS collection instrument consists of collection area with a funnel in front. The idea is to collect as much dust as possible. The instrument is designed to be located on the top deck of the rocket payload so that dust particles in the atmosphere reach the instrument as part of the airflow.

- The air flow slows down and air density increases in the vicinity of the rocket and in the instrument.

- Drag force on the dust particles changes their trajectory. Dust particles that hit the funnel fragment and some of the fragments reach the collection area.

- Closing mechanism require a small collection area, while at the same time we want to collect as much dust as possible. This can be facilitated by using a funnel.
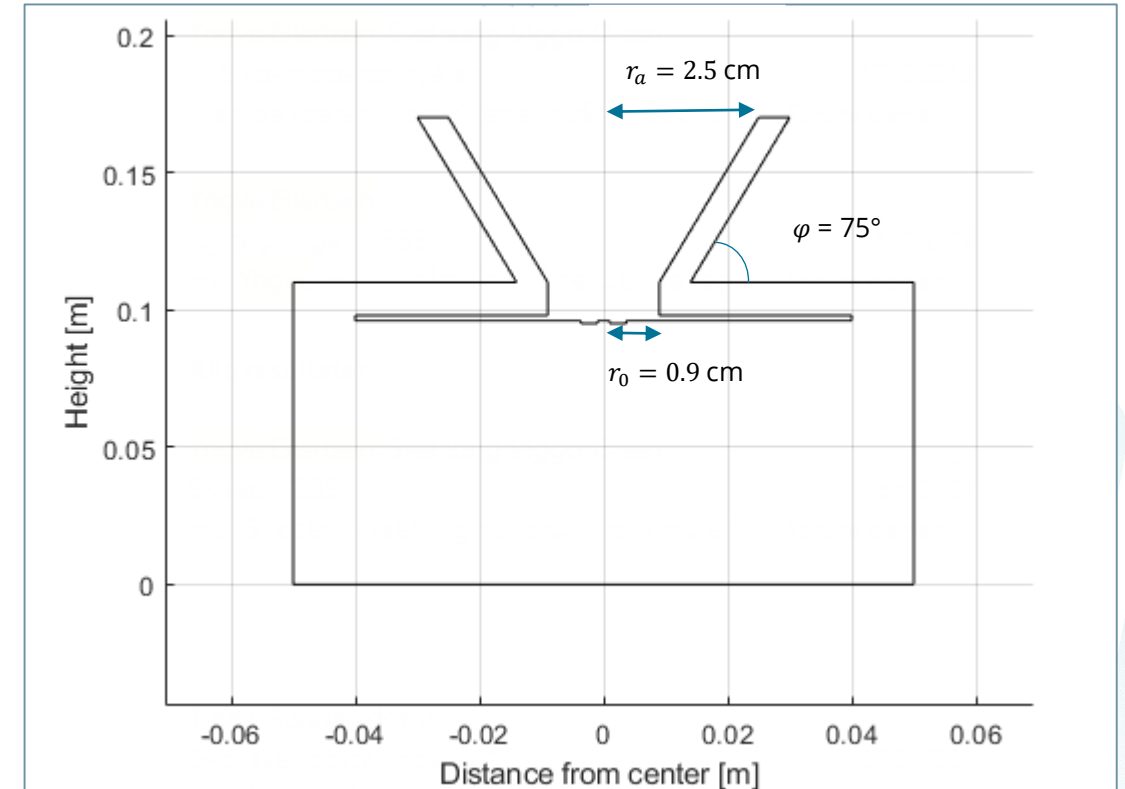
Collecting area $A_{coll} = \pi r_0^2$ = 2.55 cm²
Aperture area $A_a = \pi r_f^2$ = 19.6 cm²
Funnel angle φ = 75°
The funnel increases the sampling area by a factor of 7.7.

Model

To investigate how the particles move and are affected by the background conditions we have conducted simulations on the background airflow and particle trajectories.

- Background air flow simulated using the Monte Carlo based DS2V program (Bird 1994).

- Particle drag from method presented in Antonsen et al. (2015).

$$F_{g,d} = \pi r_d^2 m_g n_g v_{th,g}(\boldsymbol{v}_g - \boldsymbol{v}_d)\frac{1}{u}\left\{\frac{1}{\sqrt{\pi}}u\left(u + \frac{1}{2u}\right)\exp(-u^2) + \left(1 + u^2 - \frac{1}{4u^2}\right)\mathrm{erf}(u)\right\}$$

r_d, $\boldsymbol{v}_d$, is the radius and velocity of the dust particle, while $v_{th,g}, \boldsymbol{v}_g, m_g$ and n_g is the background gas parameters, u is the relative Mach number.

- Collision and fragmentation from based on work by Tomsic et al. 2013 for high velocity ice particles collision and Antonsen et al. 2017 from charged fragments in rocket experiment and Antonsen. et al 2020 on the fragmentation distribution.

Assumptions

- Axial rotational symmetry

- No angle of attack

- Spherical particles

- $m_d \gg m_g$

- Specular reflection of particles in collision

- Filling factor of 3 % of MSPs within the ice particles

- Only tracing particles fragments above 0.8 nm

- Large ice fragment of 0.5 of the initial volume survives the funnel collision.

- Distribution of the rest of the fragments follow a r^-3 distribution and are considered to be pure MSPs.

- Fragment scattering angle of 4-8 degrees from funnel wall

- 40% of the impact energy is conserved for the particles.

Model flowchart

We simulate that dust collection with two steps:
- Dust trajectories in the airflow – Primary particles

    1-9 nm : Pure MSPs

    10-50 nm: Dusty ice

- Fragmentation at funnel forms Secondary particles

Dust model assumptions:
- Small refractory particles (mesospheric smoke particles)
- Ice particles with embedded refractory particles (Polar Mesospheric cloud particles)

Flowchart of the particle motion and interaction
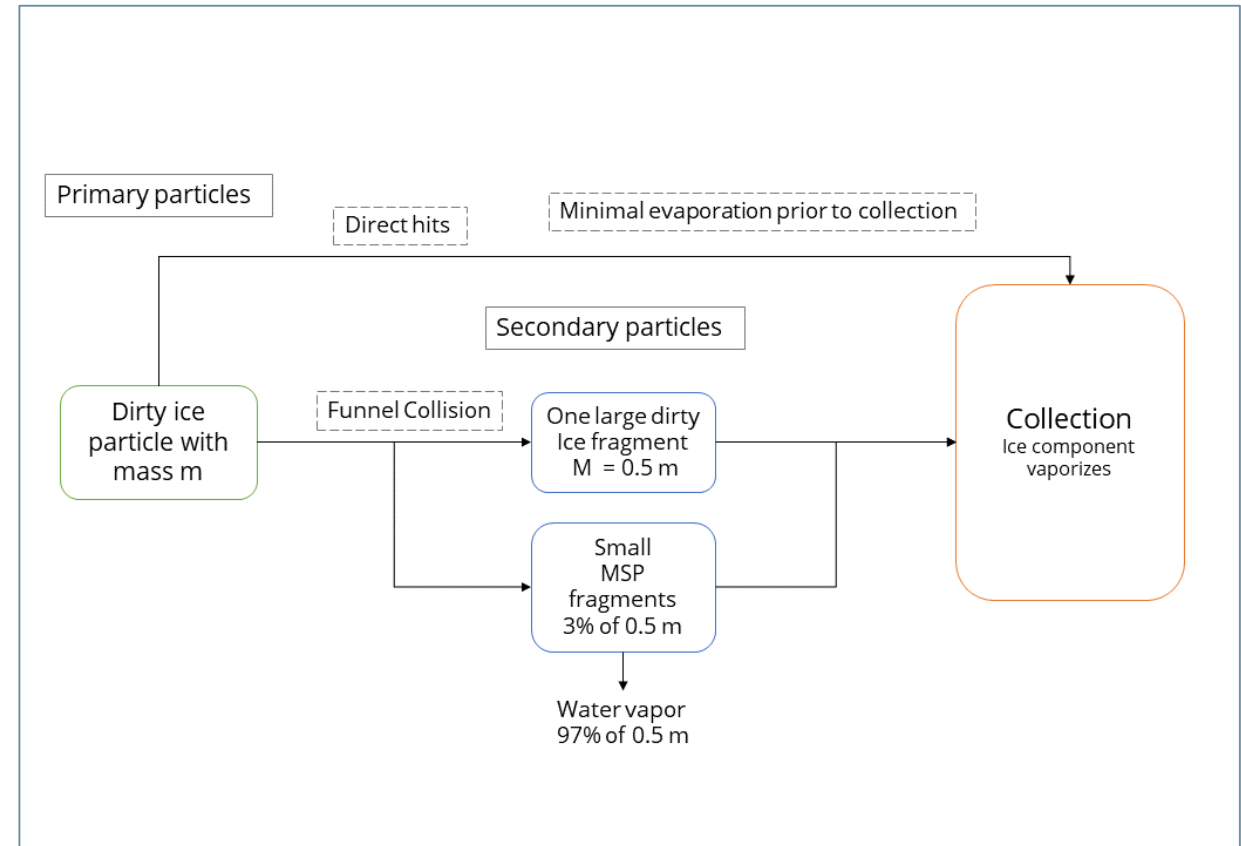
Background air flow conditions

With a rocket velocity change of 400ms^{-1} the background density within the instrument increases by over 50 %. Maximum density ~2.6 times higher at 80 km than at 85 km. The background airflow causes a drag on the particles, resulting in a deceleration of the particles which follows the expression on slide 4.
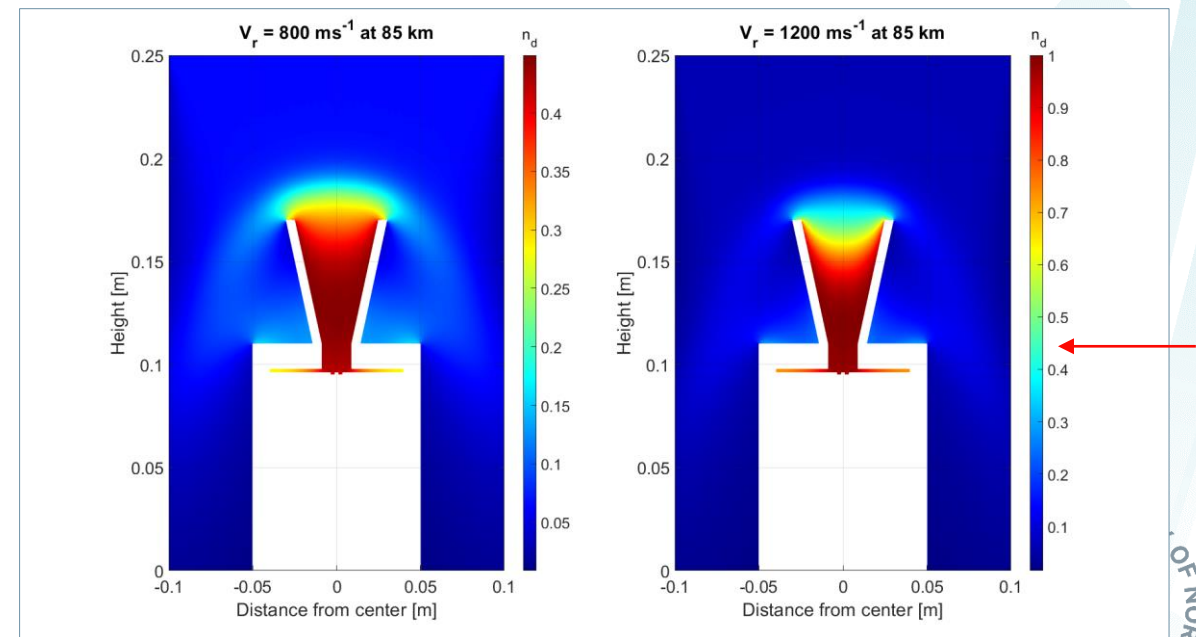
Table: Background parameters from MSIS-E-90 for 1. July 2018

|	$n_{g,0}$ [m^{-3}]	T_g [K]	$n_{g,max}$ [m^{-3}]
80 km	6.0154×10^{20}	169	9.2377×10^{21}
85 km	2.2914×10^{20}	137	3.5259×10^{21}

Altitude 80 km
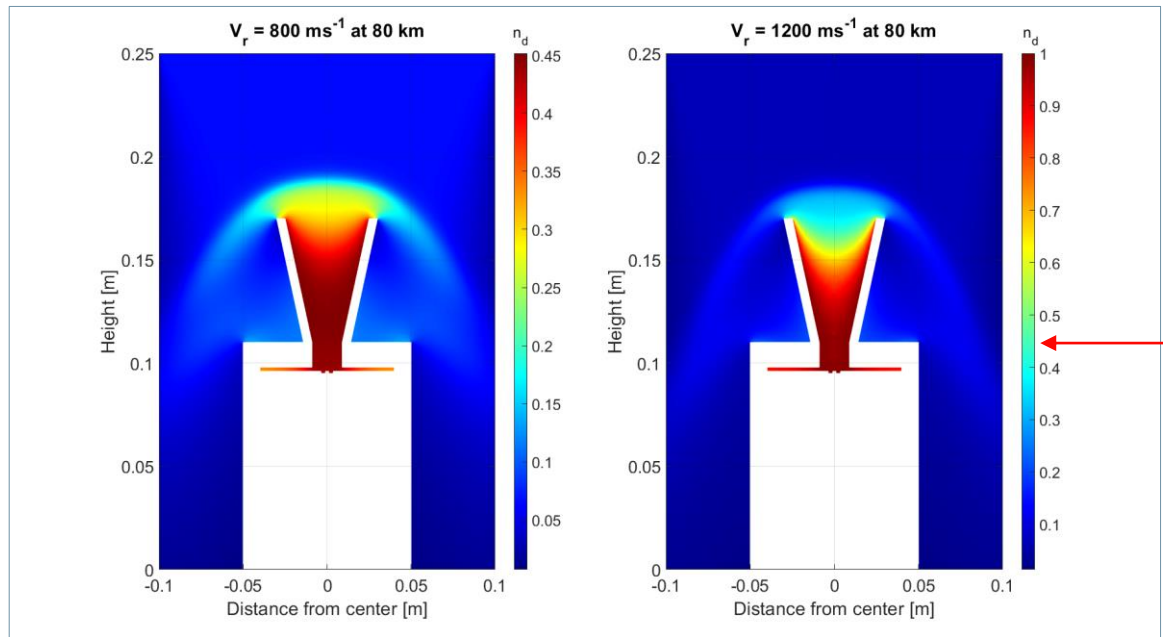
Altitude 85 km

*Note: Different color scale for the figures, arrow on left indicates maximum on right*

Deflection of primary particles in the airflow

- The instrument collects primary particles for which the collection efficiency is determined by deceleration in the airflow.

- We find that particles > 15 nm are minimally effected by the background gas, as a result of their relatively large mass.

- Simulations suggest a cut off for primary particles with radius 5 nm at 85 km and $v_r = 800$ ms^{-1} and between 10-15 nm at 80 km and $v_r = 800$ ms^{-1}.

- In terms of radial dependents, the collection efficiency decreases with distance from center, both for primary and secondary particles

- Stopping and deflection of particles < 10 nm are efficient at large distance from the center and at low altitude.

Primary particle trajectories
80 km with $v_r = 1200$ ms^{-1}
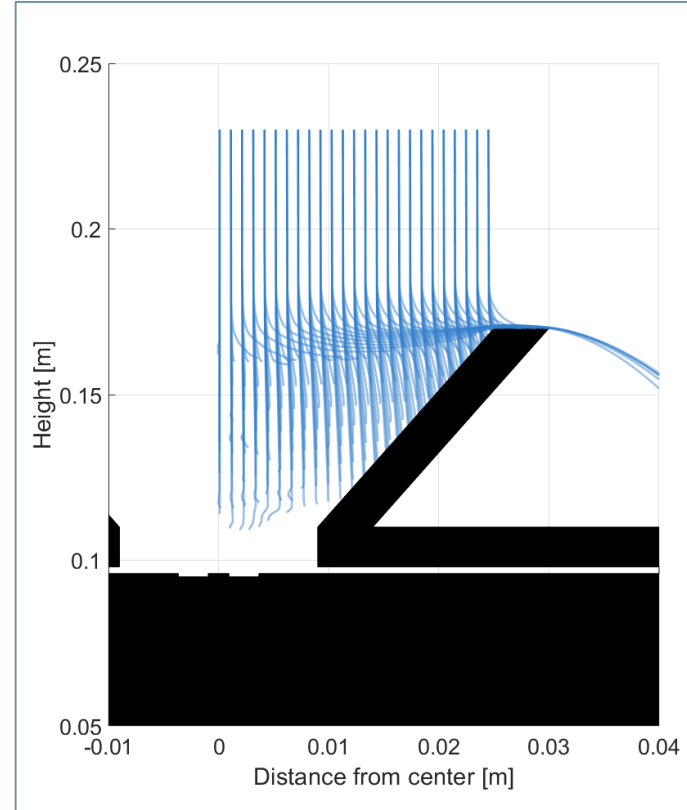
Primary particle trajectories
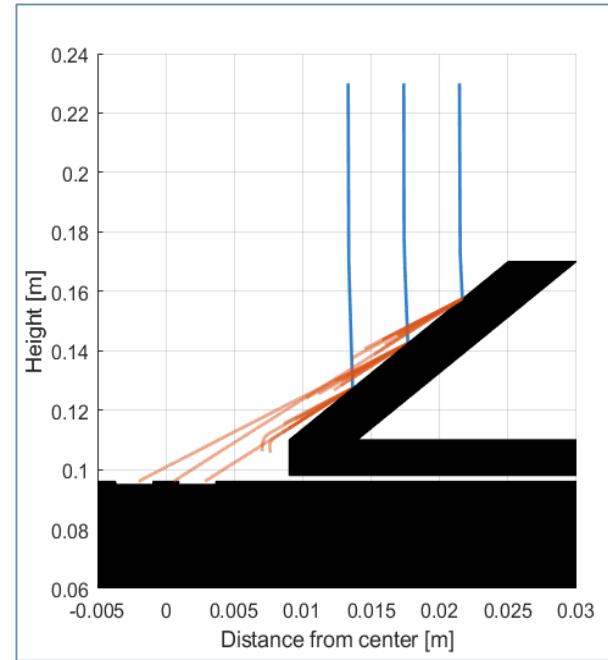85 km with $v_r = 800$ ms^{-1}
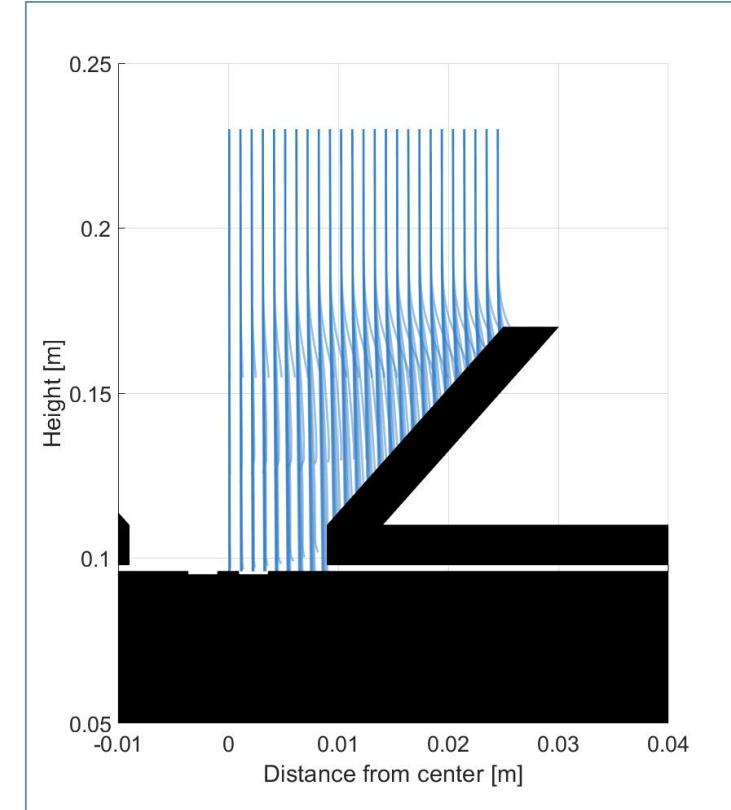
Here we see how the primary particles are affected by the neutral air conditions . The two extreme cases considered with initial particle radius in the range [1 9] nm.
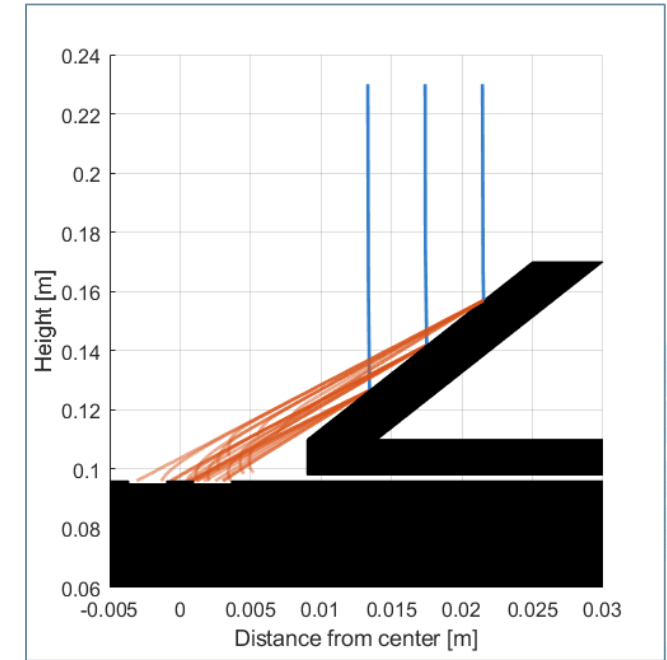
Trajectories of secondary particles

- We make the simplifying assumption that half of the particle mass is contained in a large fragment containing ice and dust.

- The other half of the mass is distributed in smaller fragments for which the ice components evaporate and only refractory particles remain.

- For the refractory particles we assume radii between 0.8 and 3 nm which is a typical size for MSP. At the same time the condition that the mass of a dust particle is large in comparison to mass of air particles is fulfilled.

- Collection efficiency for secondary particles depends on fragmentation at funnel, and motion in the airflow before and after fragmentation. Particles colliding at the top of the funnel are more strongly decelerated because they traverse a longer path through the instrument.

Secondary trajectories
80 km with $v_r = 800$ ms^{-1}

Secondary particle trajectories
85 km with $v_r = 800$ ms^{-1}

Examples of a secondary particle trajectories for a primary particle of 25 nm colliding with the funnel wall and fragmenting.

Mass Estimate

For estimation of amount of matter on the collecting area, ice particle number densities and mean radius are used from Kiliani et al. (2015)

<u>Case</u>: Altitude = 85 km, $v_r = 800$ ms^{-1}, $r_{i,d} = 25$ nm, $n_d \sim 300$ cm^{-3}, $\rho_d = 3$ $g$cm^{-3}

Primary Particle Collection (direct collection):

For a primary particle of radius 25 nm, simulations suggest a collection efficiency of ~1 at 85 km at 800 ms^{-1} . Collecting particles at a height interval of 1 km and the collection area A_{coll} (see slide 3) , the collected amount of 25 nm ice particles in the traversed volume is ~7.6e7.

Using a filling factor of 3% for the dust particle (Hervig et al. 2012), the MSP mass in the traverse volume can be found by

$$m_{collected} = A_{coll}\Delta h\, n_d 0.03\, \frac{4}{3}\pi r_{i,d}^3 \rho_d \sim 2.7 \times 10^{14} amu$$
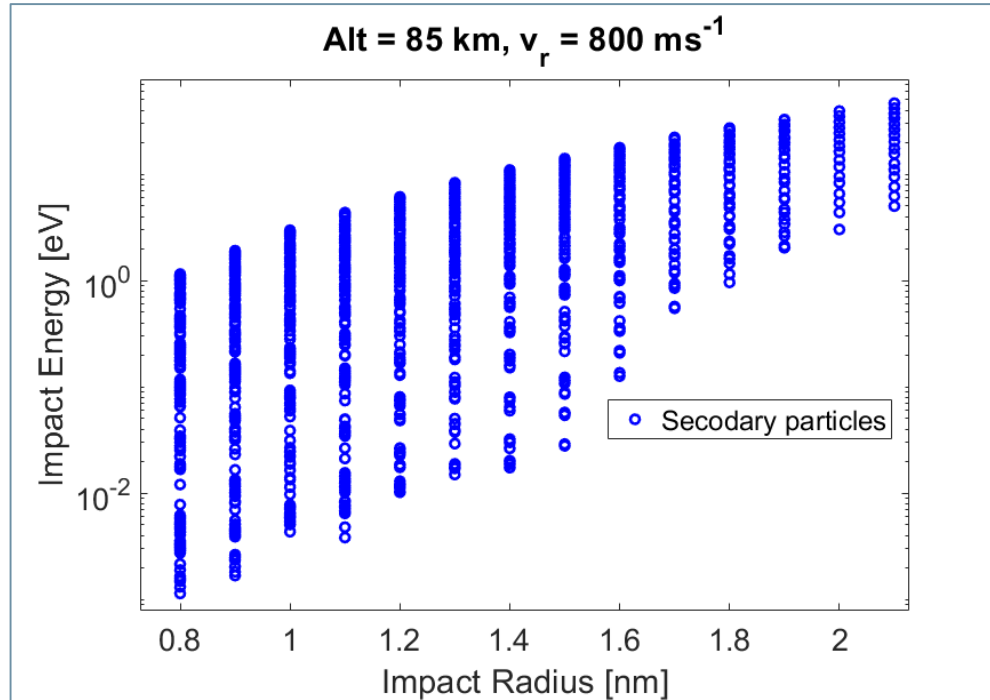
Secondary Particle Collection:

The estimate for the secondary particles is much more uncertain, since it depends on the fragmentation process. The secondary particle sampling area is $A_f - A_{coll}$ = 17.1 cm² , annular sampling area. Considering the same case as on the left hand side the estimated amount of material from secondary particle collection is

$$m_{collected} = (A_f - A_{coll})\Delta h\, n_d 0.03\, \frac{4}{3}\pi r_{i,d}^3 \rho_d \sim 1.8 \times 10^{15} amu$$

for the ideal case were all secondary particles are collected. However, as can be seen in slide 8 , not all fragments will reach the collecting surface. The volume ratio of collected MSPs vs the initial amount of MSPs indicate an efficiency of ~0.8, however this number is highly uncertain.

Impact Energy at Collection Area

Small Secondary particles reach collection are with low impact energies. The vertically aligned values indicate different energies for same fragment sizes, hence the range of impact energies for each size. The values depend on the initial fragment velocity after collision at the funnel, a parameter that has great uncertainty. Note the logarithmic y axis.
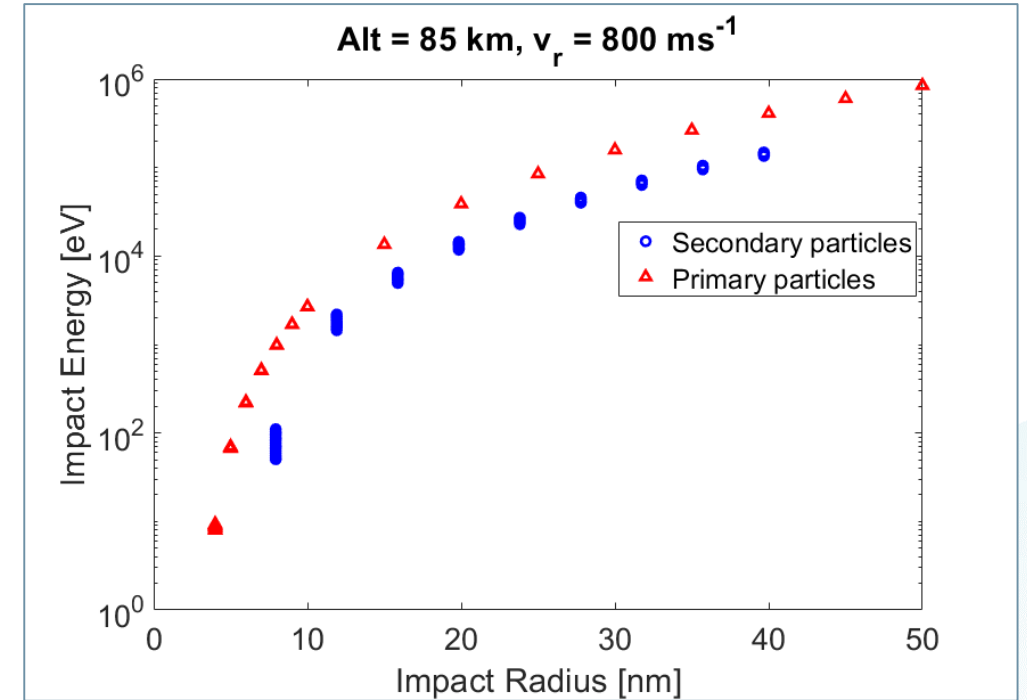
Impact energy of **large secondary particles** (blue circles) and **primary particles** (red triangles) onto the collecting area. The primary particles have energies ~5 times higher than secondary particles of similar size, as a result of the energy loss in funnel collision. We see that large particles have energies in the range of 1-6 orders of magnitude.

Discussion

- Design with the funnel increases the amount of material up to a factor of ~6.7. At the same time, there is a cut-off for small particles that will not be collected.

- The collision process at the funnel induces an uncertainty. Laboratory measurements at pure ice particles support our hypothesis that the dust particles will fragment at the funnel. We did not consider the cases that particles are reflected or sticking at the funnel surface.

- This study did not consider charge effects. Dust trajectories in the instrument can be influenced by Lorentz force. Particles can carry an initial charge and can also be charged during fragmentation. The charge can also affect the efficiency for sticking of particles to the funnel wall.

- The rocket typically has an angle of attack which was not considered here. In this case, the impact angle from the surface normal is smaller for the particles impacting on the funnel. This has an influence on the fragmentation process.

Conclusion and Future Work

Our simulations suggest that significantly higher amount of particles reach the collecting area at an altitude of 85 km in comparison to 80 km. With increasing rocket velocity the amount of background gas in the instrument increases, so that the deceleration of particles in the instrument is greater.

For particles that reach the collecting area, we find a range of impact energies between 1 eV and 10^5 eV. This is partly a result of the range of particle sizes, but also for particles of the same size the impact energies vary considerably. The impact energies will be important parameter for choosing the collecting surface so that the particles are stopped, remain on the collection surface and leave the surface intact.

Future work will involve investigation of potential collecting surfaces, contamination issues, and the lid mechanisms for the instrument.

References

Antonsen, T., & Havnes, O. (2015). On the detection of mesospheric meteoric smoke particles embedded in noctilucent cloud particles with rocket-borne dust probes. *Review of Scientific Instruments*, *86*(3), 033305.

Antonsen, T., Havnes, O., & Mann, I. (2017). Estimates of the Size Distribution of Meteoric Smoke Particles From Rocket-Borne Impact Probes. *Journal of Geophysical Research: Atmospheres*, *122*(22), 12-353.

Antonsen, Mann, Vaverka, Nouzak and Fredriksen, (2020) . Comparison of Contact Charging and Impact Ionization in Low Velocity Impacts: Implications for Dust Detection in Space. Submitted ANGEO.

Bird, G. A., & Brady, J. M. (1994). *Molecular gas dynamics and the direct simulation of gas flows* (Vol. 42). Oxford: Clarendon press.

Havnes, O., Antonsen, T., Hartquist, T. W., Fredriksen, Å., & Plane, J. M. C. (2015). The Tromsø programme of in situ and sample return studies of mesospheric nanoparticles. *Journal of Atmospheric and Solar-Terrestrial Physics*, *127*, 129-136.

Hervig, M. E., Deaver, L. E., Bardeen, C. G., Russell III, J. M., Bailey, S. M., & Gordley, L. L. (2012). The content and composition of meteoric smoke in mesospheric ice particles from SOFIE observations. *Journal of atmospheric and solar-terrestrial physics*, *84*, 1-6.

Kiliani, J., Baumgarten, G., Lübken, F. J., & Berger, U. (2015). Impact of particle shape on the morphology of noctilucent clouds. *Atmospheric Chemistry and Physics*, *15*, 12897-12907.

Tomsic, A., Andersson, P. U., Marković, N., & Pettersson, J. B. (2003). Collision dynamics of large water clusters on graphite. *The Journal of chemical physics*, *119*(9), 4916-4922.

Acknowledgements